SUPPLEMENTARY MATERIAL

An Integrated Strategy for Pre-Disposal of Spent Cation-Exchange Resins by Repurposing Industrial By-Products

Francesco Galluccio[1], Andrea Santi[1], Edoardo Rizzi[1], Fabio Fattori[1], Gabriele Magugliani[1], Veronica Piazza[2], Chiara Milanese[3], Giacomo Diego Gatta[4], Luca Fornara[5], Elena Macerata[1], Mario Mariani[1], Eros Mossini[1]*

[1]Laboratory of Radiochemistry and Radiation Chemistry, Department of Energy, Politecnico di Milano, via La Masa 34, 20156 Milano, Italy

[2]Laboratory of Catalysis and Catalytic Processes, Department of Energy, Politecnico di Milano, via La Masa 34, 20156 Milano, Italy

[3]Hydrogen Laboratory, Department of Chemistry, University of Pavia & C.S.G.I., Viale Taramelli 16, 27100 Pavia, Italy

[4]Department of Earth Sciences, University of Milan, Via S. Botticelli 23, 20133 Milano, Italy

[5]Joint Research Centre, European Commission, Via E. Fermi 2749, 21027 Ispra, Italy

*Corresponding author, e-mail: eros.mossini@polimi.it

1. Characterization of materials

1.1. Cationic resin

Table S1: Technical datasheet for Amberlite IRN 77 provided by the supplier.

	IRN 77
Physical form	Amber beads
Functional group	Sulfonic acid
Delivered ionic form	H^+
Particle size (mm)	0.6-0.7
Cross-linking (DVB) (%)	8
Total exchange capacity (eq/L)	≥1.90
Moisture content (wt%)	49-55

1.2. Catalysts and precursors

1.2.1. XRF analysis

Table S2: Chemical composition (wt.%) of the catalysts and of the powdery precursors of the alkali-activated matrix.

Material	SiO_2	Al_2O_3	K_2O	Fe_2O_3	CaO	MnO	H_2O
VT	57.3 ± 0.5	17.8 ± 0.3	7.0 ± 0.1	5.7 ± 0.2	8.3 ± 0.3	0.2 ± 0.1	0.9 ± 0.1
BFS	26.1 ± 0.1	5.9 ± 0.1	0.5 ± 0.1	0.7 ± 0.1	40.3 ± 0.1	< 0.1	< 0.1
CFA	59.0 ± 0.2	21.3 ± 0.1	3.3 ± 0.1	8.1 ± 0.1	3.9 ± 0.1	< 0.1	< 0.1
EAFS	11.7 ± 0.2	3.6 ± 0.1	0.0 ± 0.1	40.0 ± 0.2	33.2 ± 0.1	4.1 ± 0.1	< 0.1

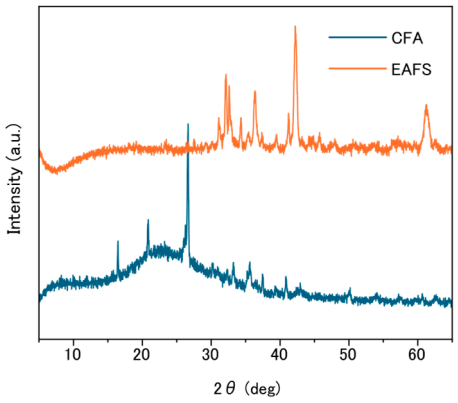

Figure S1: X-ray diffraction patterns (Cu-Kα rad.) of the catalysts. The Bragg peaks related to the inorganic species have been assigned as reported in the text.

The diffraction patterns show medium-high fractions of either amorphous or microcrystalline phases, with few broad Bragg peaks attributable, for CFA, to dominant quartz SiO_2 and subordinate mullite $Al_{4+2x}Si_{2-2x}O_{10-x}$ (with x within 0.17 to 0.59), hematite Fe_2O_3 and lime CaO, and, for EAFS, to wüstite FeO and larnite Ca_2SiO_4.

1.2.2. SEM analysis

The SEM micrographs point out the typical morphology of both CFA and EAFS [39,40]: spheres of 1-100 μm in diameters for the most part for CFA, and edgy-shaped particles due to the crushing and milling for EAFS, with dimensions less than 100 μm.

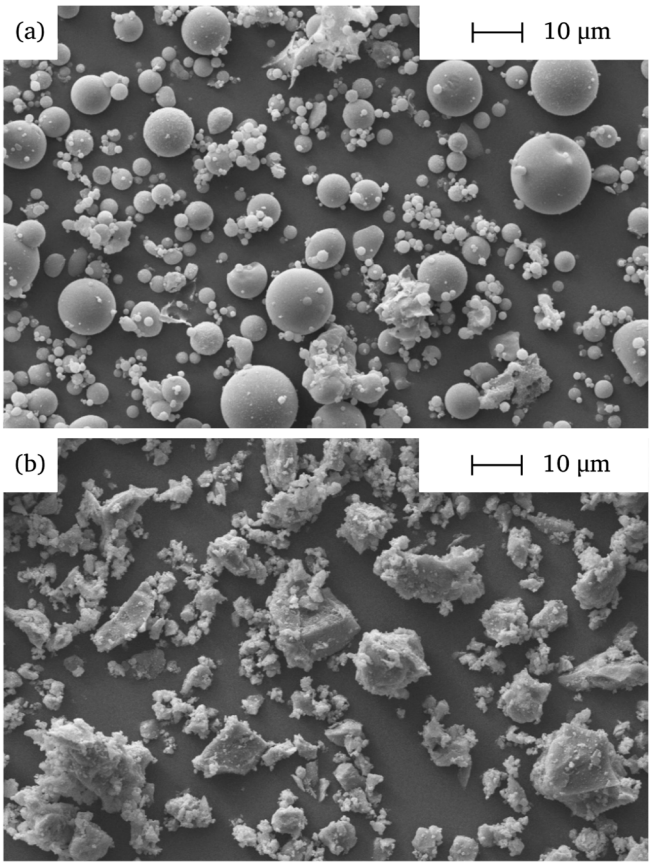

Figure S2: SEM micrographs of the catalysts: (a) CFA; (b) EAFS.

1.2.3. Nitrogen adsorption-desorption analysis

The specific surface area of the electric arc furnace slag (EAFS) is 1.53 ± 0.01 m^2/g, with pore volumes of 0.03 cm^3/g, while for the coal fly ash (CFA) the values are 7.09 ± 0.07 m^2/g and 0.02 cm^3/g, respectively.

1.3. Liquor (Gas Chromatography-Mass Spectrometry)

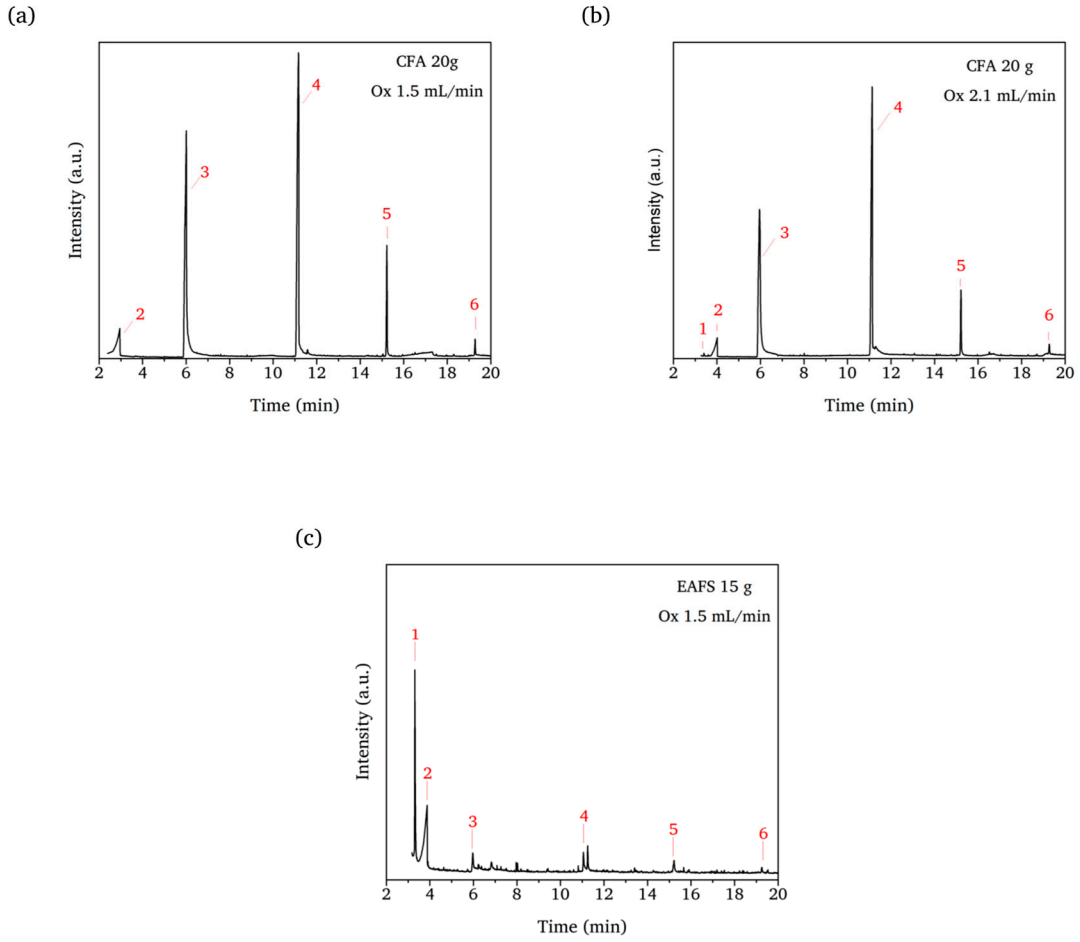

Figure S3: GC-MS chromatograms of samples with different amount of CFA, EAFS, and oxidant. Identified species: 1) oxalic acid ($C_2H_2O_4$) + formic acid (CH_2O_2); 2) acetic acid ($C_2H_4O_2$); 3) cyclotrisiloxane, hexamethyl- (Silox-3, $C_6H_{18}O_3Si_3$); 4) cyclotetrasiloxane, octamethyl- (Silox-4, $C_8H_{24}O_4Si_4$); 5) cyclopentasiloxane, decamethyl- (Silox-5, $C_{10}H_{30}O_5Si_5$); 6) cyclohexasiloxane, dodecamethyl- (Silox-6, $C_{12}H_{36}O_6Si_6$).

Table S3: Percentage peak areas calculated in GC-MS chromatograms of samples at different amount of catalyst and oxidant.

Catalyst	Catalyst mass	Oxidant	*Percentage Peak Area (%)*					
	(g)	(mL/min)	*Oxalic acid + Formic acid*	*Acetic acid*	*Silox-3*	*Silox-4*	*Silox-5*	*Silox-6*
CFA	20	1.5	--	7.2	38.6	46.5	6.9	0.8
CFA	20	2.1	0.2	5.3	40.5	46.9	6.3	0.8
CFA	25	2.1	0.1	4.6	46.2	42.5	5.9	0.6
EAFS	15	1.5	28.7	47.3	5.4	13.3	3.8	1.5
EAFS	15	2.1	4.6	18.1	40.6	31.9	4.2	0.6

2. Materials and methods

2.1. Fenton-like wet oxidation

Proof of concept (10 g)

The first parameters to be analyzed were the ones related to the initial conditions, such as initial temperature and pH. Regarding the start-up temperature, previous experiments excluded starting at room or lower temperatures, and a range up to around 70 °C was considered. Additionally, experiments were conducted both by keeping the heating power throughout the process or by removing it after reaching the start-up temperature. Concerning the pH, despite the optimal range from 2.7 to 3.5 proposed by Zahorodna et al. [43], there is no unique reference to optimize the process, and for several experiments pH is reported at circumneutral [44] or very acidic values [17-18,41]. The pH is known to affect the speciation [26,42] and solubility of iron: sub-optimal iron speciation results in the inhibition of Fe(II) regeneration and consequent interruption of the reaction due to its unavailability. Furthermore, the presence of organic intermediates of degradation can enhance iron precipitation at circumneutral pH values, also influencing the choice of acid to use for pH regulation [4,19,20]. Considering this issue, a range between 1 and 2 was adopted, adjusting the pH value with addition of concentrated sulfuric acid if necessary.

Regarding the catalysts, different amounts of CFA and EAFS were tested. A theoretical maximum value for both the materials was calculated from literature, in which 0.1-0.3 M iron sulfate solutions were widely used in homogeneous conditions [13,14,17,18, 41]. Therefore, the iron content of the 0.2 M solution was considered as reference for the initial estimation of the heterogeneous catalyst to be employed, resulting in 8.6 g CFA and 2.3 g EAFS. Then, the amounts to be tested were chosen considering the iron content of the two catalysts, in order to obtain comparable results.

Two different oxidant rates were tested: 0.6 mL/min and 0.8 mL/min, with the latter obtained by the experiment in homogeneous conditions [13]. The oxidant rate was set at the beginning of the reaction, once the start-up temperature was reached, and was kept constant throughout the process. Various reaction times, which, in turn, mean various total oxidant amounts, were tested (2.0, 2.5, 3.0, and 4.5 hours) with the final goal of minimizing it.

3. Results and discussion

3.1. Fenton-like wet oxidation

Proof of concept (10 g)

During small-scale tests, a comparable evolution of the mixture was observed with both catalysts. The initial solution was gray (CFA) or black (EAFS) depending on the catalyst color. In correspondence of the peak of temperature, as reported in Figure S4 for both the catalysts, bubbles appeared contributing to the movement of the spent ion-exchange resins (SIERs) beads. At the same time, the color of the solution became dark brown with a lighter brown surface layer. After the peak temperature, the mixture remained brown in the bulk with a gold-yellow top layer, which is consistent with the complete dissolution of the IER as reported in literature [4, 13,17]. During the remaining time to the end of the reaction, namely from around 30 minutes to 180 minutes, the mixture became progressively yellow in the bulk with a white top layer. The process reactivity, visible throughout the reaction in the form of small bubbles, vanished towards the end. At the end of the treatment towards room temperature, the solution was yellow and clear, with a dark precipitate on the bottom of the flask, mainly ascribable to the spent catalyst. Hence, the evolution of temperature and colour over time could be used for the monitoring of the treatment process.

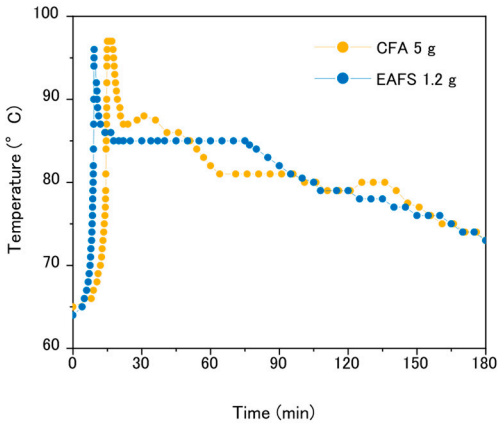

Figure S4: Comparison between the temperature profiles of the best conditions found with 5 g CFA and 1.2 g EAFS as catalyst and 0.6 mL/min of oxidant rate at the proof-of-concept scale.

Start-up temperature and pH

The selection of the start-up temperature has been heavily influenced by the previous experiment performed in homogeneous conditions [13], in fact it was seen that starting from room temperature (or slightly above) resulted in an excess of reactivity and less controllable process. A starting temperature of 65 ± 2 °C was finally chosen. The heating power was kept constant throughout the process. Indeed, it was found that the suspension right after achieving the startup temperature inhibited the trigger of the reaction and induces an incomplete mineralization of the resin beads. In the starting pH range tested, i.e., from 1 to 2, no appreciable modifications have been found. Therefore, the initial conditions have been set at 65 ± 2 °C and pH 1.5.

Oxidant rate and reaction time

Based on previous experimental findings, a range of 0.6-0.8 mL/min of oxidant rate was investigated by keeping constant the total reaction time. No remarkable differences were found in the behavior of the reaction that resulted in a complete dissolution of the cationic resin beads, and comparable WRR values. Hence, the 0.6 mL/min injection rate was chosen as optimal condition, thereby minimizing the oxidant consumption.

Maintaining constant the oxidant rate, different reaction times were tested. For instance, it was noted that the extension from 2.5 to 4.5 hours did not lead to further improvements of the process. Conversely, decreasing the reaction time from 2.5 to 2.0 hours resulted in an incomplete decomposition of organic matter, resulting in a turbid solution and in turn in bad residues with low WRR values. The selected reaction time of 3.0 hours was sufficient to ensure reaching the final temperature plateau.

Catalyst type and mass

For both the catalysts, an increase in the time to reach the maximum temperature has been found when the catalyst mass was decreased. In general, the reactions catalyzed by EAFS were faster, having times to reach the peak temperature (t_{peak}) shorter than the ones with CFA at similar iron content. Moreover, the reactions with EAFS showed a narrower and steeper peak followed by a temperature plateau (Figure S4), instead of a wider peak followed by a slower temperature decrease via multiple plateaus.

Especially using CFA catalyst at decreasing mass, a widening of the region at maximum temperature, which is the region of maximum reactivity, was observed (Figure S5), along with a cyclical behavior, which was compatible with the iron regeneration redox cycle.

For the two catalysts, values of Weight Reduction Ratio (WRR) above 60% were reached. The slightly better performance of EAFS resulting in drier final residue can be probably ascribed to the different size and nature of the spent catalyst powders, remaining in the final residue. The results hereby discussed are reported in Table S4.

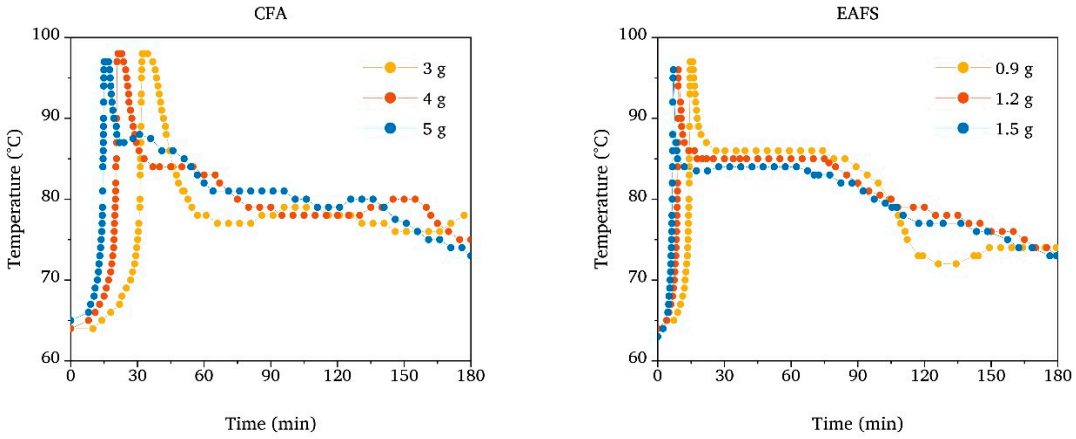

Figure S5: Temperature profiles found with different catalyst masses, when treating 10 g of SIERs with 0.6 mL/min of oxidant rate: (left) CFA; (right) EAFS.

Table S4: Main results obtained in the proof-of-concept experiments with different catalyst type and mass, and oxidant rate of 0.6 mL/min.

Catalyst	Catalyst mass (g)	Fe content (g)	t_{peak} (min)	WRR_{org} (%)
CFA	3.0	0.20	32 ± 1	61 ± 1
	4.0	0.26	21 ± 1	61 ± 1
	5.0	0.32	15 ± 1	63 ± 1
EAFS	0.9	0.22	15 ± 1	62 ± 1
	1.2	0.29	9 ± 1	65 ± 1
	1.5	0.36	7 ± 1	65 ± 1

Drying process

The drying process was generally performed over 8 hours. The residue obtained with CFA had the consistence of a dark gray paste (Figure S6a); on the other hand, the residue obtained with EAFS (Figure S6b) resulted in a light gray sand with fine grains, still easily workable.

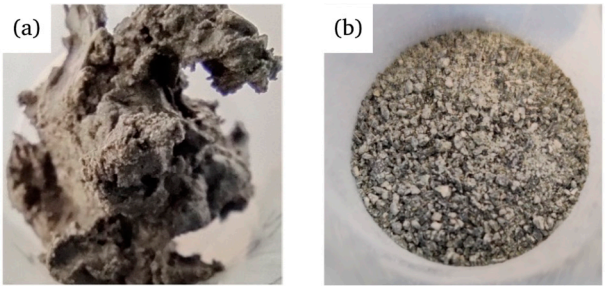

Figure S6: Residues obtained at the end of the Fenton-like treatment with different catalysts: a) CFA; b) EAFS.

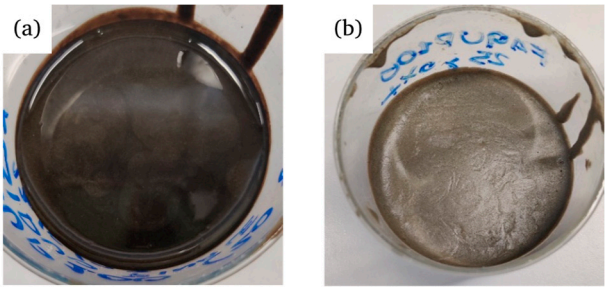

Figure S7: Residues obtained with same CFA catalyst mass at increasing oxidant rates: a) 1.5 mL/min; b) 2.2 mL/min.

3.2. Conditioning in alkali-activated matrix

3.2.1. Characterization of residues

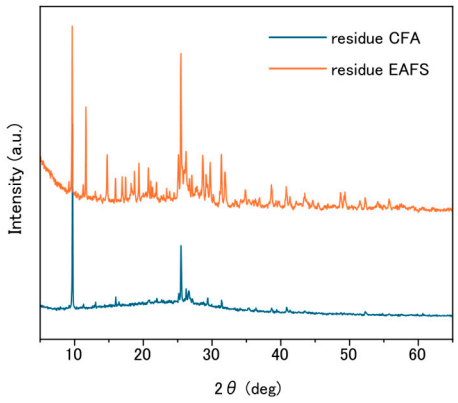

Figure S8: X-ray diffraction patterns (Cu-Kα rad.) of the residues obtained downstream of Fenton treatment, evaporation and drying for tests run in optimal conditions. The Bragg peaks related to the inorganic species have been assigned as reported in the text.

3.2.2. Production of waste forms

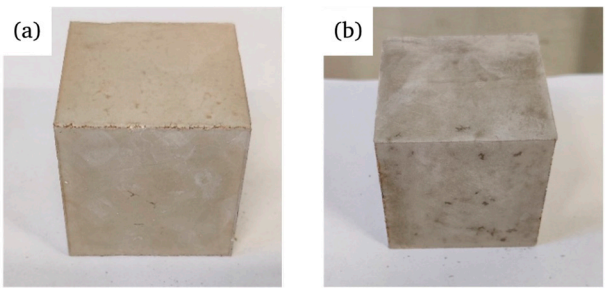

Figure S9: Specimens for compressive strength at 28 days of curing: a) 6 wt.% loading of EAFS-based residue; b) 6 wt.% loading of CFA-based residue.